

Received April 1, 2019, accepted May 28, 2019, date of publication June 5, 2019, date of current version June 21, 2019.

Digital Object Identifier 10.1109/ACCESS.2019.2920845

# Improving the Signal-to-Noise Ratio of Underground Nuclear Magnetic Resonance Data Based on the Nearby Reference Noise Cancellation Method

JIAN ZHANG, GUANFENG DU<sup>1</sup>, JUN LIN, XIAOFENG YI, AND CHUANDONG JIANG<sup>2</sup>

College of Instrumentation and Electrical Engineering, Jilin University, Changchun 130061, China

Key Laboratory of Geophysics Exploration Equipment, Ministry of Education of China, Jilin University, Changchun 130061, China

Corresponding author: Chuandong Jiang (chuandongjiang@gmail.com)

This work was supported in part by the National Science Foundation of China under Grant 41604083 and Grant 2011YQ030133, in part by the Natural Science Foundation of Jilin Province under Grant 20190201111JC and Grant 20170520164JH, and in part by the Fundamental Research Funds for the Central Universities.

**ABSTRACT** Surface and underground nuclear magnetic resonance (UNMR) method has the advantage of direct and quantitative detection of groundwater and has been widely used in water resource survey and advance detection of water sources causing disaster in underground space. However, the UNMR signal is extremely weak in tunnels or mines. The signal-to-noise ratio (SNR) of received data at one single record is even less than  $-20$  dB because of the strong environmental noise. A nearby reference noise cancellation (NRNC) method is proposed in this study to improve SNR. The method calculates the transfer function between the reference coil and the detection coil by using the second half of the received data to determine the noise estimation in the first half of the detection coil. The non-linear fitting method is used to estimate and remove the UNMR signal in the noise estimation and avoid the loss of the UNMR signal in the detection coil. We compare the nearby reference coil layouts of coaxial, non-separation tri-axial, and separation tri-axial types, as well as the NRNC results of the number and distance of different reference coils, through a large number of experiments. The non-separation tri-axial reference coil is optimal. The experimental results show that the SNR can be increased significantly by 18.1 dB, and the uncertainty in UNMR signal parameter estimation is evidently decreased. We prove that the NRNC algorithm is superior to the existing remote reference noise cancellation and power frequency modeling algorithms, and discuss that the improvement in SNR will be beneficial to improve the accuracy of inversion results.

**INDEX TERMS** Nuclear magnetic resonance, signal-to-noise ratio, reference noise cancellation, nearby reference coil.

## I. INTRODUCTION

Nuclear magnetic resonance (NMR) is a new and highly potential geophysical method for exploring groundwater [1]. Compared with other geophysical prospecting methods for indirect water detection, the greatest advantage of the NMR method is that it can directly prove the existence of groundwater and quantitatively describe water content [2]. The NMR method can be divided into two application fields: surface and underground. The detection of subsurface aquifers, caverns, and pipelines on the ground belongs to the conventional

surface NMR. In underground spaces, such as tunnels or mines, the detection of water-bearing structures in front of or around the working face belongs to the newly developed underground NMR (UNMR) [3].

Compared with laboratory applications, such as NMR spectroscopy and Magnetic Resonance Imaging (MRI), the UNMR applications under the earth's surface are more difficulties and challenges [4], [5]. First, the background magnetic field is small. Medium-high magnetic field ( $0.1 - 7$  Tesla) is used by NMR spectroscopy and MRI, whereas the earth's magnetic field ( $B_0 = 2.5 - 6.5 \times 10^{-6}$  Tesla) is used by UNMR [6]. The amplitude of the UNMR signal is proportional to the square of the background

The associate editor coordinating the review of this manuscript and approving it for publication was Fang Yang.

magnetic field; thus, the UNMR signal is extremely weak at only the level of nanovolt [7], [8]. Second, the coil for receiving is small in size. Surface NMR generally uses a square coil with a length of 100 m to receive signals [1]. Owing to space constraints, UNMR only uses coils with lengths of 2 – 6 m [9], and the effective area and the signal amplitude are smaller than those in surface applications. Third, the underground space environment noise is large. NMR spectroscopy and MRI work in a shielded environment with minimal noise. By contrast, UNMR works in the field with difficult-to-shield environmental noise. In the underground, considerable electrical equipment is needed, and the environmental noise is high [8]. Therefore, the data signal-to-noise ratio (SNR) obtained by UNMR is low at less than –20 dB. Some scholars believe that UNMR signal is completely submerged in noise, and reliable detection cannot be achieved [7]. With the improvement in measuring instruments [8], [9], many scholars have detected UNMR signals in tunnel and mine environments, but the extremely low SNR remains a significant challenge faced by UNMR.

Noise in NMR received data is divided into spikes, power-line harmonics, and random noise [10]. Many scholars have proposed various elimination methods for these noises. Spikes refer to short-lived and extremely large noise, which can be eliminated by statistical criteria [11], energy operators [12], and spike modeling [13]. The power line harmonic noise is a noise composed of multiple harmonics with a power line (50 or 60 Hz) as the base frequency. Harmonic modeling [10] and adaptive noise cancellation [10], [14] can be used to eliminate power line harmonics. The random noise is generally considered subject to Gaussian distribution, and can thus be decreased by stacking or weighted stacking [15], or the NMR signal is extracted directly from random noise using empirical modal decomposition or singular spectral analysis [16], [17].

However, a large number of measured data in tunnels and mines indicate that an uncertain system noise remains in the UNMR received data, which may be caused by a complex noise source or internal instrument. Although the noise is random, it cannot be decreased by superposition. Reference [18] used a three-direction reference coil and reference noise cancellation (RNC) [12], [19] to eliminate the correlated noise (harmonics and uncertain system noise) in the detection coil. The method requires the reference coil to keep away from the detection coil to prevent coupling the UNMR signal. When using the RNC method, the UNMR signal is considered correlated noise, which results in a loss of useful signals. Nevertheless, as the distance between the coils increases, the correlation of noise and the effect of the RNC decrease [20]. The remote reference coil is consequently difficult to apply when making measurement in a small underground space.

To address the contradiction between the noise correlation of the reference coil and the loss of UNMR signal, a nearby RNC (NRNC) method is proposed in this study. First, we design three nearby reference coil layouts of coaxial,

non-separation tri-axial, and separation tri-axial types. Second, the RNC method is improved to adapt to the nearby reference coils. Although the reference coil receives the UNMR signal, it will not lose the UNMR signal in the detection coil. Third, we compare the effects of the number, distance, and direction of the reference coil on the SNR enhancement, and determine the optimal nearby reference coil layout. Finally, the advantages of the proposed method and the influence of SNR enhancement on the inversion results are discussed by a comparison with the existing method of harmonic modeling and the remote RNC.

## II. PRINCIPLES AND METHODS

### A. UNMR SIGNALS AND NOISE

The UNMR principle states that when the hydrogen proton in groundwater is excited, its spin rotating axis is deflected, which causes the NMR phenomenon [21]. After the excitation stops, the coil receives a free-inductive decay signal, that is, the UNMR signal [2], which can be expressed as

$$V_{\text{NMR}} = V_0 e^{-t/T_2^*} \cos(2\pi f_L t + \varphi_0) \quad (1)$$

where  $V_0$  is called the initial amplitude of the UNMR signal, which is proportional to the water content of groundwater;  $T_2^*$  is the average relaxation time (it is equal to the transverse relaxation time  $T_2$  when the magnetic field is uniform), which is related to the pore distribution of the aqueous medium;  $f_L$  is the Larmor frequency, which is proportional to  $B_0$  of the measuring location, and  $f_L = \gamma B_0$ ;  $\gamma$  is the hydrogen proton gyromagnetic ratio; and  $\varphi_0$  is the initial phase, which is related to the resistivity of the underground medium, the deviation of the transmitting and receiving frequencies, and the shape and position of the coil [22].

The received data contain strong noise due to the effect of the construction environment. The noise can be divided into spikes  $V_{\text{spike}}$ , harmonics  $V_{\text{harmonic}}$ , and random noise  $V_{\text{random}}$  depending on the frequency and amplitude characteristics.  $V_{\text{random}}$  can be divided into Gaussian random noise  $V_{\text{gauss}}$  and uncertain systematic noise  $V_{\text{uncertain}}$ , where  $V_{\text{uncertain}}$  refers to the combination of non-Gaussian noise in the environment and noise inside the instrument system. Therefore, the received data are expressed as

$$V_{\text{R}} = V_{\text{NMR}} + V_{\text{spike}} + V_{\text{harmonic}} + V_{\text{uncertain}} + V_{\text{gauss}} \quad (2)$$

$V_{\text{uncertain}}$  is a non-Gaussian distribution, which is not compensated; therefore, it cannot be decreased by superposition.

### B. NEARBY REFERENCE COIL

In surface measurement, the laying of multiple remote reference coils is usually used, as shown in Fig. 1a. The reference coils 1–3 must be kept away from the detection coil, with the distance more than 1.5 times longer than the size of the detection coil [12]. In underground measurement, the sizes of the detection coil and reference coil are very small because of the effective space, and the same plane is difficult to pave in the form of a multi-directional distal distribution,

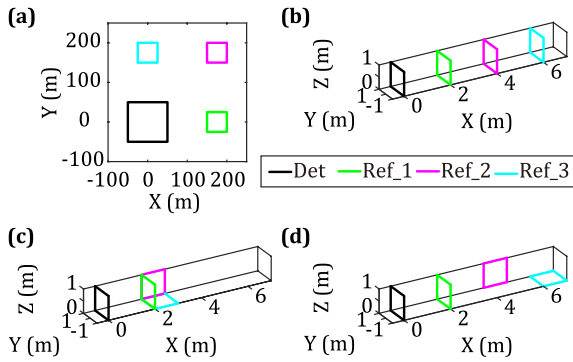


**FIGURE 1.** Surface NMR remote reference coil and three types of UNMR nearby reference coil. (a) Remote reference coil, (b) Coaxial nearby reference coil, (c) Non-separation tri-axial nearby reference coil, and (d) Separation tri-axial nearby reference coil.

as shown in Fig. 1. In this study, three types of multi-nearby reference coil suitable for underground space are designed. They are coaxial, non-separation tri-axial, and separation tri-axial types, as shown in Figs. 1b, c, and d, respectively. The coaxial type adopts a plurality of reference coils, which is placed with the detection coil coaxial and distributed at equal distances to receive noise data from different positions. The non-separation tri-axial type uses a reference coil in three directions (coaxial, horizontal, and vertical) to receive noise data in three directions. The separation tri-axial type is based on the non-separation tri-axial. Each coil is separated by a distance, and six types exist based on the three directions of the different combinations, one of which is shown in Fig. 1d. The UNMR signal is introduced in the reference coil because the reference coil is close to the detection coil; thus, the conventional RNC algorithm must be improved.

**C. NEARBY REFERENCE NOISE CANCELLATION METHOD**

$V_{spike}$ ,  $V_{harmonic}$ , and  $V_{gauss}$  in the received data refer to (2) are eliminated or decreased by the different processing methods mentioned above, and the methods used in this study are mainly for  $V_{harmonic}$  and  $V_{uncertain}$ . The UNMR signal is exponentially attenuated following (1). Although the received data in the reference coil contain the UNMR signal, the UNMR signal in the second half of the data has been significantly attenuated. First, a certain distance exists between the reference coil and detection coil; if coupled with the UNMR signal, then the amplitude is also less than the signal in the detection coil. Second, the relaxation time of the UNMR signal is generally 0.05 – 0.4 s, and the data acquisition time is 1 s. At the beginning of the second half of 0.5 s, the signal amplitude has been attenuated to the original 0.000045–0.29. Therefore, this study assumes that no UNMR signal exists in the second half of the reference coil data, or that its effect can be ignored.

The NRNC algorithm is shown in Fig. 2 (taking three reference coils as an example), and the specific steps for implementation are described as follows:

- 1) The received data of the detection coil and all reference coils are divided into the first and second halves based on time, respectively.
- 2) The data of the first and second halves are grouped (usually  $N = 10$  groups) into discrete Fourier transforms [19]. The frequency domain data of the  $n$ th group in the first half of the reference coils are  ${}^1R_1(n, \omega)$ ,  ${}^1R_2(n, \omega)$ , and  ${}^1R_3(n, \omega)$ ; the frequency domain data of the  $n$ th group in the second half of the reference coil are  ${}^2R_1(n, \omega)$ ,  ${}^2R_2(n, \omega)$ , and  ${}^2R_3(n, \omega)$ ; and the frequency domain data of the  $n$ th group in the second half of the detection coil are  ${}^2S(n, \omega)$ .
- 3) For each frequency point  $\omega_i$ , the correlation between the detection coil and reference coil can be expressed as [19]

$$S_2 = R_2 H \tag{3}$$

where  $S_2 = [{}^2S(1, \omega_i), {}^2S(2, \omega_i), \dots, {}^2S(N, \omega_i)]^T$ ,

$$R_2 = \begin{bmatrix} {}^2R_1(1, \omega_i) & {}^2R_2(1, \omega_i) & {}^2R_3(1, \omega_i) \\ {}^2R_1(2, \omega_i) & {}^2R_2(2, \omega_i) & {}^2R_3(2, \omega_i) \\ \vdots & \vdots & \vdots \\ {}^2R_1(N, \omega_i) & {}^2R_2(N, \omega_i) & {}^2R_3(N, \omega_i) \end{bmatrix},$$

$H = [H_1(\omega_i), H_2(\omega_i), H_3(\omega_i)]^T$  is a transfer function and T is the transpose symbol. The least squares method is used to solve (3) to obtain

$$H = (R_2^T R_2)^{-1} R_2^T S_2 \tag{4}$$

- 4) Following the calculation to obtain the transfer function  $H$ , the first half of the reference coils  ${}^1R_1(n, \omega)$ ,  ${}^1R_2(n, \omega)$ , and  ${}^1R_3(n, \omega)$ , and the frequency domain data  $U$  of the noise estimation in the detection coil

$$U = R_1 H \tag{5}$$

$U$  is made inverse discrete Fourier transform to obtain the time domain data  $u(t)$ .

- 5) Whether an UNMR signal exists in  $u(t)$  is judged as follows: if it does not exist, then the detection coil received data  $s(t)$  are used to subtract  $u(t)$  to obtain the data after noise cancellation; if it exists, then the UNMR signal parameters are estimated by the non-linear fitting method and are decreased in  $u(t)$ , and then  $s(t) - u(t)$ .

For the fitting method of the UNMR signal, the Hilbert transform and a low-pass filter are first used to obtain the complex envelope of the signal [23], that is

$$V_{NMR}^c(t) = V_0 e^{-t/T_2^*} [\cos(2\pi df t + \varphi_0) + j \cos(2\pi df t + \varphi_0)] \tag{6}$$

where  $df = f - f_L$  is the frequency offset and  $j$  is the imaginary unit. The non-linear fitting method [24] is used to estimate  $V_0$ ,  $T_2^*$ ,  $df$ , and  $\varphi_0$ . In step 5), the noise estimation using all the reference coils' data  $u(t)$  is used to fit UNMR signal. The received data of each reference coil  $s(t)$  are not used

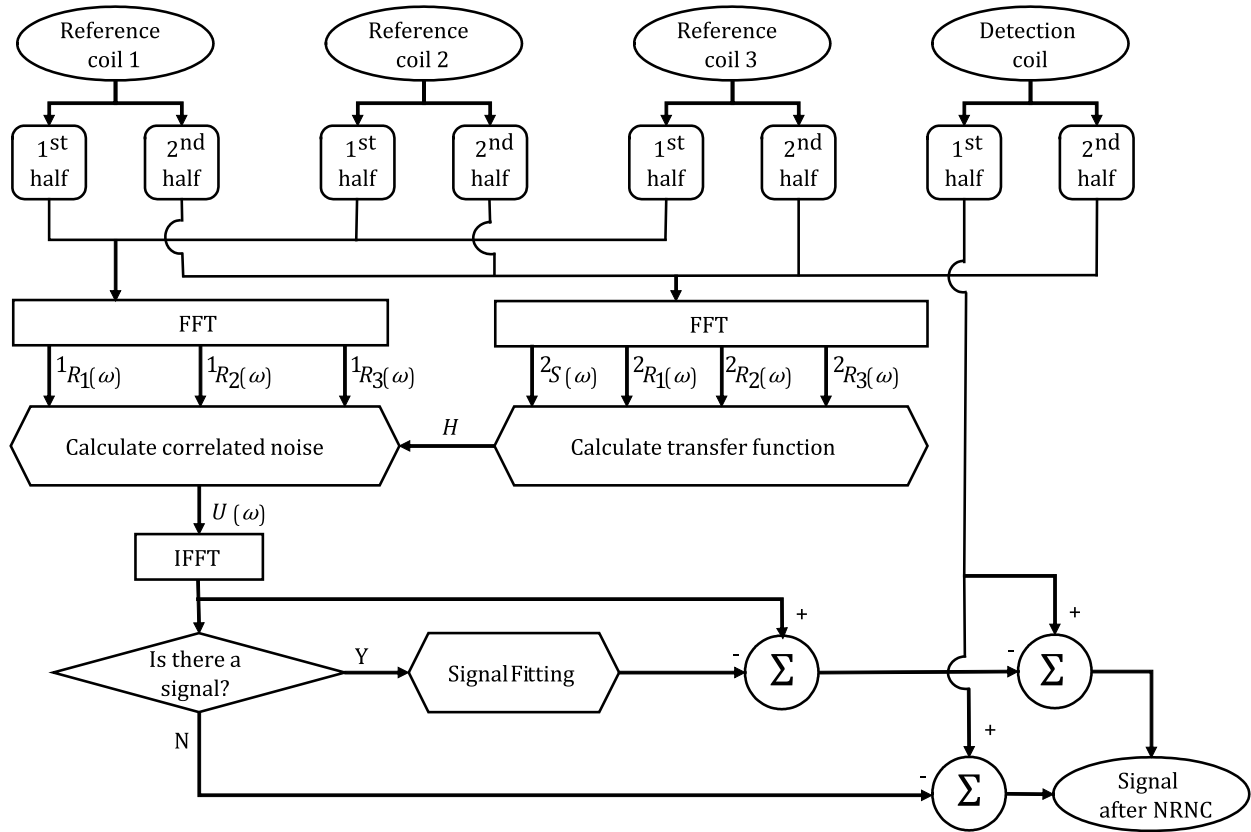


FIGURE 2. Schematic of the Nearby Reference Noise Cancellation (NRNC) algorithm.

because  $u(t)$  does not contain random noise, the synthesized UNMR signal is large, and the fitting accuracy is high.

In summary, the NRNC algorithm in Fig. 2 uses the second half of the UNMR-free signal to calculate the transfer function, and then uses the first half of the data to calculate the noise estimate and remove the UNMR signal. Therefore, the NRNC is able to eliminate most of the correlated noise without losing the UNMR signal. Moreover, compared with the complexity of the traditional RNC algorithm, only the steps of segmentation and nonlinear fitting are added, and the calculation speed is equivalent.

### III. RESULTS

#### A. SYNTHETIC RESULTS OF NRNC

Synthetic data are used to perform simulation experiments for verifying the effectiveness of the noise cancellation method based on the multi-nearby reference coil proposed in this study. The synthetic data include the four components of  $V_{\text{UNMR}}$ ,  $V_{\text{harmonic}}$ ,  $V_{\text{uncertain}}$ , and  $V_{\text{gauss}}$ , as shown in Fig. 3a, and their spectrums are shown in Fig. 3b. The parameters of the UNMR signal are  $e_0 = 500$  nV,  $T_2^* = 200$  ms,  $f_L = 2325$  Hz, and  $\varphi_0 = 3/\pi$  rad. The base frequency of  $V_{\text{harmonic}}$  changes randomly in the  $50 \pm 0.02$  Hz range (Gaussian distribution), and the number of harmonics is 100 [10]. The amplitude of each harmonic varies randomly within the

0 – 1000 nV range (evenly), and the phase varies randomly between  $-\pi$  and  $\pi$  (evenly).  $V_{\text{uncertain}}$  is from the results extracted from measured data, and its mean square root amplitude, that is, the noise level, is 1256 nV. The noise level of  $V_{\text{gauss}}$  is 500 nV. The sampling rate of the simulation data is 25 kHz, and the acquisition time is 1 s. In Fig. 3a,  $V_{\text{harmonic}}$  and random noise are only one example, each with a different measurement result.

In the detection coil, the received data include all of the above mentioned signals and noise. The time domain and spectrum signals are shown in Figs. 3c, and d, respectively. In Fig. 3c, the UNMR signal (red line) in the observed data is completely submerged by ambient noise, and the SNR is  $-23.5$  dB. For three reference coils, UNMR signals exist in the received data in addition to ambient noise because they are near the detection coil. Therefore, 0.5, 0.2, and 0.1 times of the UNMR signal are added to the reference coils 1, 2, and 3, respectively, to simulate the nearby reference coil. The base frequency of the three reference coils is the same,  $V_{\text{harmonic}}$ , but the amplitude and phase of each harmonic are not equal, nor  $V_{\text{gauss}}$ . For  $V_{\text{uncertain}}$ , different examples of noise level are added to the three reference coils, and the noise level is randomly generated.

A noise cancellation processing of the synthesized data is conducted in Fig. 4 on the basis of the use of the NRNC

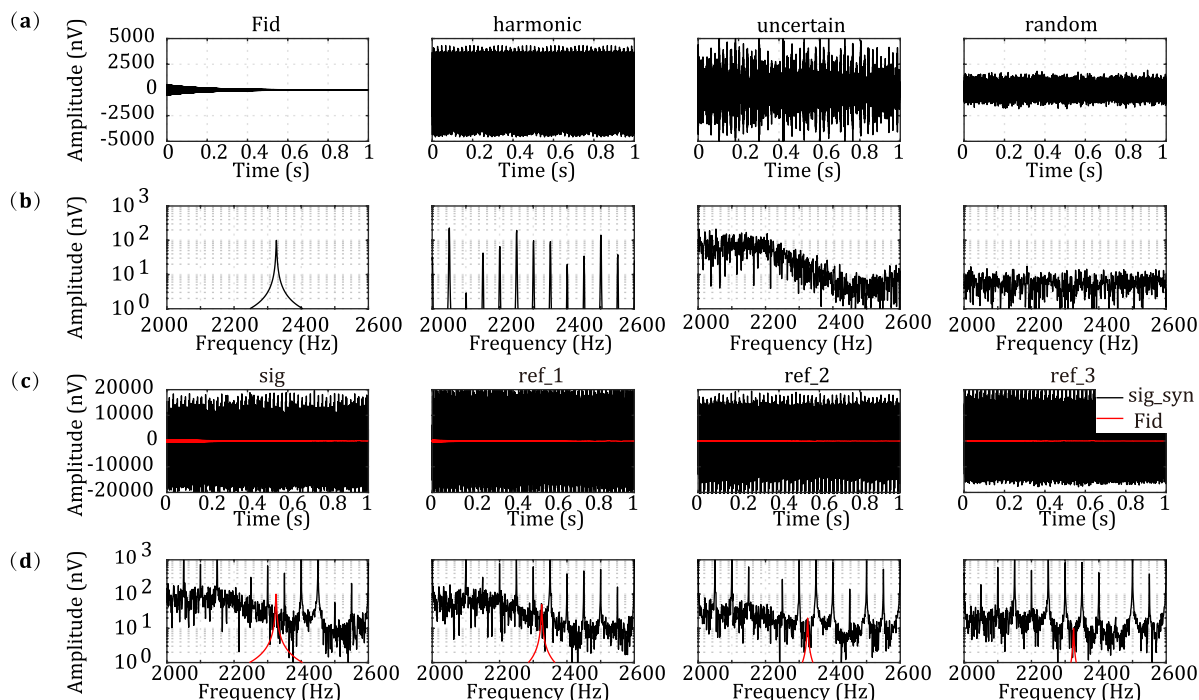


**FIGURE 3.** Synthetic data for NRNC simulation experiments. (a)  $V_{NMR}$ ,  $V_{harmonic}$ ,  $V_{uncertain}$ , and  $V_{gauss}$ . (b) Corresponding spectrum. (c) Received data in detection coil (sig), reference coil 1 (ref\_1), reference coil 2 (ref\_2), and reference coil 3 (ref\_3). (d) Corresponding spectrum.

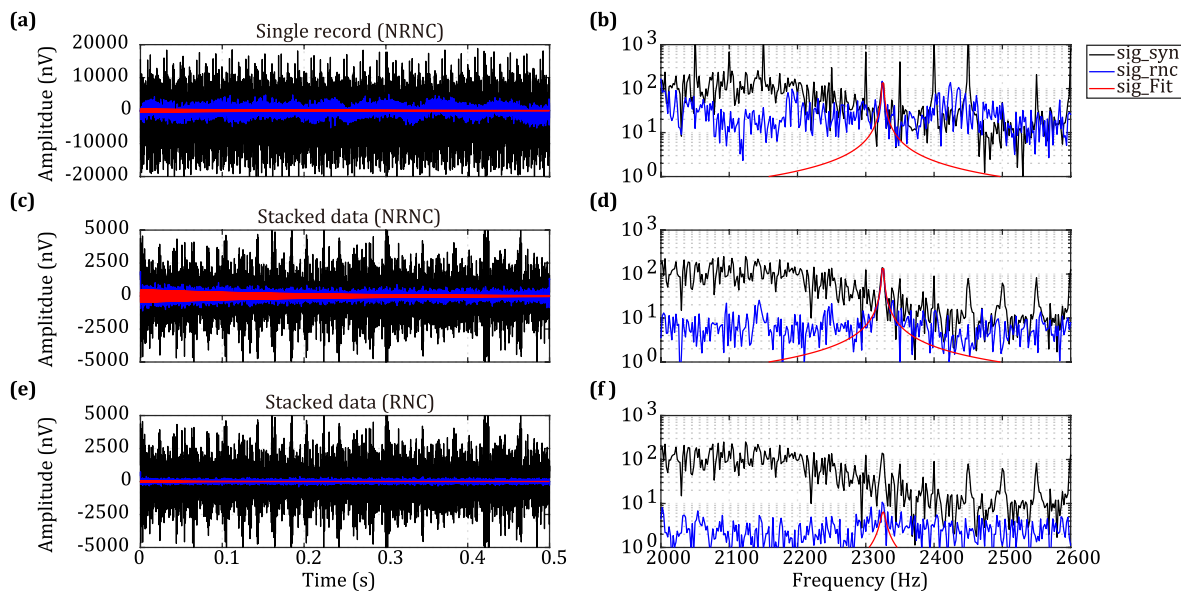


**FIGURE 4.** NRNC processing results and comparison with conventional RNC results. (a) Single data after NRNC processing. (b) Corresponding spectrum. (c) Stack data after NRNC processing. (d) Corresponding spectrum. (e) Stack data after conventional RNC processing. (f) Corresponding spectrum.

algorithm described in subsection II-C, as shown in Fig. 2. In Fig. 4a, the blue curve shows the result of NRNC noise cancellation, and its noise level is significantly smaller than that before processing. The red curve shows the UNMR signal after fitting. The SNR after calculation is  $-8.8$  dB, which

is increased by  $14.7$  dB. The spectrum analysis results of Fig. 4b show that the NRNC processing not only eliminates  $V_{harmonic}$  but also greatly reduces the noise level of the uncertain system. Moreover, the amplitude of the frequency point corresponding to the UNMR signal remains the same.



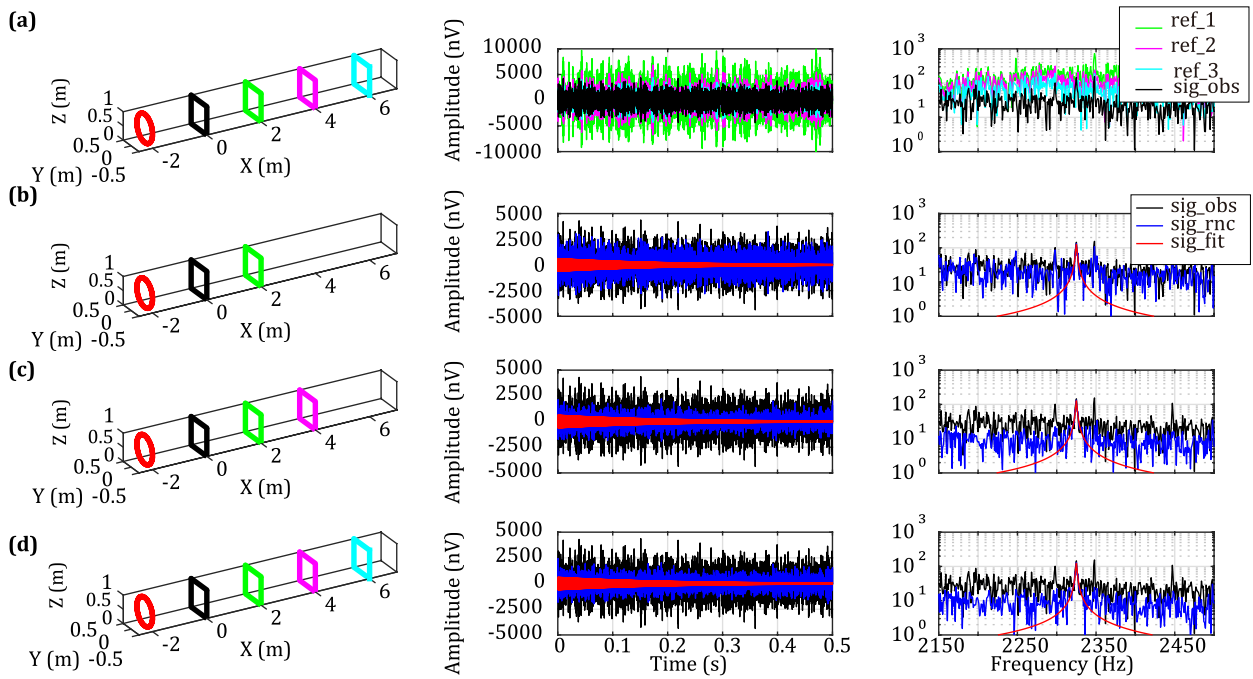


**FIGURE 5.** NRNC processing results of coaxial reference coil. (a) Reference coil layout, received data, and corresponding spectrum. (b) Single reference coil layout, NRNC processing results, and corresponding spectrum. (c) Double reference coil layout, NRNC processing results, and corresponding spectrum. (d) Triple reference coil layout, NRNC processing results, and corresponding spectrum.

However, the SNR of single observation data remains low, at which pointing that the data contain random noise. We therefore repeat the production of 64 sets of observational data and then conduct NRNC processing and stack processing, as shown in Figs. 4c, and d. The SNR after stack processing is 7.0 dB, and the amount of stack data that have not been processed by NRNC is -9.9 dB. Consequently, the SNR is increased by 16.9 dB. At this time, the UNMR signals in the data are fitted to obtain  $\hat{e}_0 = 497.2 \pm 6.9$  nV and  $\hat{T}_2^* = 201.9 \pm 4.2$  ms.

The processing results of the NRNC algorithm are compared with the conventional RNC results to verify its accuracy, as shown in Figs. 4e, and f. The conventional RNC processing results can also eliminate  $V_{\text{harmonic}}$  and  $V_{\text{uncertain}}$  but cause a serious loss to the UNMR signal (red curve). After the data processed and fitted, the  $\hat{e}_0 = 65.5$  nV and  $\hat{T}_2^* = 50$  ms, and the results have been completely deviated from the simulation parameters. The reason is that the UNMR signal in the detection coil is eliminated as the related noise after RNC processing because of the existence of the UNMR signal in the reference coil. Therefore, Fig. 4 shows that, when the reference coil is close to the detection coil, the NRNC algorithm must be used to ensure the accuracy of the detection of the UNMR signal.

### B. NRNC PROCESSING RESULTS OF MEASURED DATA OF COAXIAL REFERENCE COIL

A test platform is established in the laboratory to conduct acquisition and noise cancellation experiments using multiple

reference coil types shown in Fig. 1 for verifying the NRNC processing effect of the actual data acquisition. Fig. 5 depicts the experimental result of a coaxial reference coil. The red coil in Fig. 5a is a transmitting coil that uses arbitrary signal generation instruments (Tektronix AFG3022C) to produce 1 V UNMR signals, in which  $T_2^* = 200$  ms,  $f_L = 2325$  Hz, and  $\varphi = 0$  rad. After a resistance in series and space attenuation of the transmitting coil, the UNMR signal sensing within the detection coil (black) 2 m away is approximately 660 nV. The UNMR signal is completely submerged in noise because of the large amount of ambient noise of approximately  $10^4$  nV. The received data and their spectrum are shown in the black curve in Fig. 5a.

The green, purple, and cyan coils are the reference coils 1, 2 and 3, respectively, at a distance of 2 m. The received data and spectrum of these coils are shown in the corresponding color curves in Fig. 5a. The above mentioned data are the results after 64 repeated acquisition and stack processing.

Single, double, and triple reference coils are used to conduct NRNC processing on the received data of the detection coil. The processing results and spectrum are shown in Figs. 5b, c, and d. The noise level  $N_{\text{obs}}$  and SNR for the measurement data, the noise level  $N_{\text{RNC}}$  and SNR' after NRNC processing, the SNR increase value, UNMR signals  $\hat{e}_0$ , and the estimated values  $\hat{T}_2^*$  are shown in Table. 1. Figs. 5b, c, and d show that, as the number of reference coils increases, the noise level after NRNC processing gradually decreases. Therefore, the increase in the number of reference coils can significantly improve SNR and then promote the

**TABLE 1. NRNC processing result statistics of coaxial reference coil.**

Reference coil	$N_{obs}$ (nV)	$N_{RNC}$ (nV)	SNR (dB)	SNR' (dB)	$\Delta$ SNR (dB)	$\hat{e}_0$ (nV)	$\hat{T}_2^*$ (ms)
1	1174.5	781.1	-5.1	-1.6	3.5	$666.1 \pm 32.8$	$261.8 \pm 21.3$
2		856.4		-2.4	2.7	$670.3 \pm 36.1$	$258.9 \pm 23.0$
3		841.4		-2.2	2.9	$670.7 \pm 34.1$	$258.9 \pm 21.7$
1 and 2		460.3		3.0	8.1	$690.0 \pm 17.0$	$252.1 \pm 10.2$
1 and 3		549.9		1.5	6.6	$676.5 \pm 22.6$	$257.6 \pm 14.2$
2 and 3		628.2		0.3	5.4	$657.4 \pm 25.7$	$267.4 \pm 17.4$
1, 2, and 3		377.8		4.7	9.8	$661.2 \pm 16.2$	$251.5 \pm 9.7$

**TABLE 2. NRNC processing result statistics of tri-axial reference coil.**

Reference coil	$N_{obs}$ (nV)	$N_{RNC}$ (nV)	SNR (dB)	SNR' (dB)	$\Delta$ SNR (dB)	$\hat{e}_0$ (nV)	$\hat{T}_2^*$ (ms)
a	1162.1	442.5	-5.0	3.3	8.5	$662.3 \pm 20.7$	$219.3 \pm 9.5$
		323.6		6.1	11.1	$658.8 \pm 14.0$	$220.3 \pm 6.5$
		319.8		6.2	11.2	$666.8 \pm 13.9$	$217.6 \pm 6.3$
		194.0		10.5	15.5	$650.5 \pm 8.4$	$213.2 \pm 4.0$
		176.0		11.3	16.3	$651.0 \pm 7.8$	$213.1 \pm 3.7$
		221.7		9.3	14.3	$640.4 \pm 8.3$	$206.4 \pm 4.1$
		123.2		14.4	19.4	$653.2 \pm 4.9$	$202.4 \pm 2.5$
b	1201.4	284.5	-5.3	7.2	12.5	$671.7 \pm 13.7$	$206.4 \pm 7.4$
c	1192.3	303.4	-5.3	6.6	11.9	$682.8 \pm 14.7$	$238.7 \pm 11.0$
d	1250.0	277.1	-5.7	7.4	13.1	$647.2 \pm 13.8$	$196.2 \pm 5.4$

accuracy of the UNMR signal  $\hat{e}_0$  and estimated  $\hat{T}_2^*$ , as shown in Table. 1. Table. 1 shows that, in single reference coil, the processing results using reference coil 1 is better than that using reference coils 2, and 3. For double reference coils, the processing results using reference coils 1, and 2 is better than that using reference coils 1, and 3, and reference coils 2, and 3. The reason is that, in addition to the number of reference coils, the distance between the reference coil and detection coil is an important factor that affects the processing results of NRNC. Reference coils 2, and 3 are far from the detection coil; therefore, they have limited contributions to the elimination of ambient noise. The UNMR signal fitting using reference coils 2, and 3 is identical.

**C. NRNC PROCESSING RESULTS OF MEASURED DATA OF TRI-AXIAL REFERENCE COIL**

The same UNMR signal generator and processing method as in subsection III-B are used to test the NRNC processing effect of the tri-axial reference coil. Three reference coils are located at 2 m away from the detection coil to consider the layout of non-separation tri-axial reference coil, and their processing results are shown in Fig. 6a and Table. 2. The processing results of Fig. 6a and the results of spectrum analysis indicate that the non-separation tri-axial reference coil is significantly better than the coaxial reference coil. This result is reflected by the lower residual noise level and higher SNR of the former than the latter. The conclusions obtained from the statistical analysis of the processing results in Table. 2 are similar to those in Table. 1, that is, the SNR promotion

and accuracy of the estimation of  $\hat{e}_0$  and  $\hat{T}_2^*$  increase significantly with the increase in the number of reference coils. The difference is that the non-separation tri-axial reference coil obtains noise data from three directions. Each direction has an attenuation effect on the noise of the detection coil. Consequently, the processing results of the double or triple reference coil are better than those of the coaxial reference coil.

The non-separation tri-axial reference coil is close to the detection coil, which utilizes the advantage of strong correlation. The tri-axial reference coil is separated to form a combination of three different direction reference coils to test the noise cancellation effect of the tri-axial and coaxial reference coils, as shown in Figs. 6b, c, and d. The statistics of the processing results in Fig. 6 and Table. 2 shows that  $V_{harmonic}$ ,  $V_{uncertain}$ , and  $V_{gauss}$  present relatively large changes in the data measured at different times. However, a comparison of the  $\Delta$ SNR in Tables 1 and 2 shows that the processing results of the three types of separation tri-axial reference coil are poorer than that of the non-separation tri-axial reference coil but are significantly better than that of the coaxial reference coil. The non-separation tri-axial reference coil is better than the separation tri-axial reference coil when using a single reference coil because of the mutual inductance between the reference coils, and the single axial reference coil is coupled with other two axial noise, such as reference coil 1. Therefore, the direction, number, and distance of the nearby reference coil are important factors that affect the processing results of NRNC.

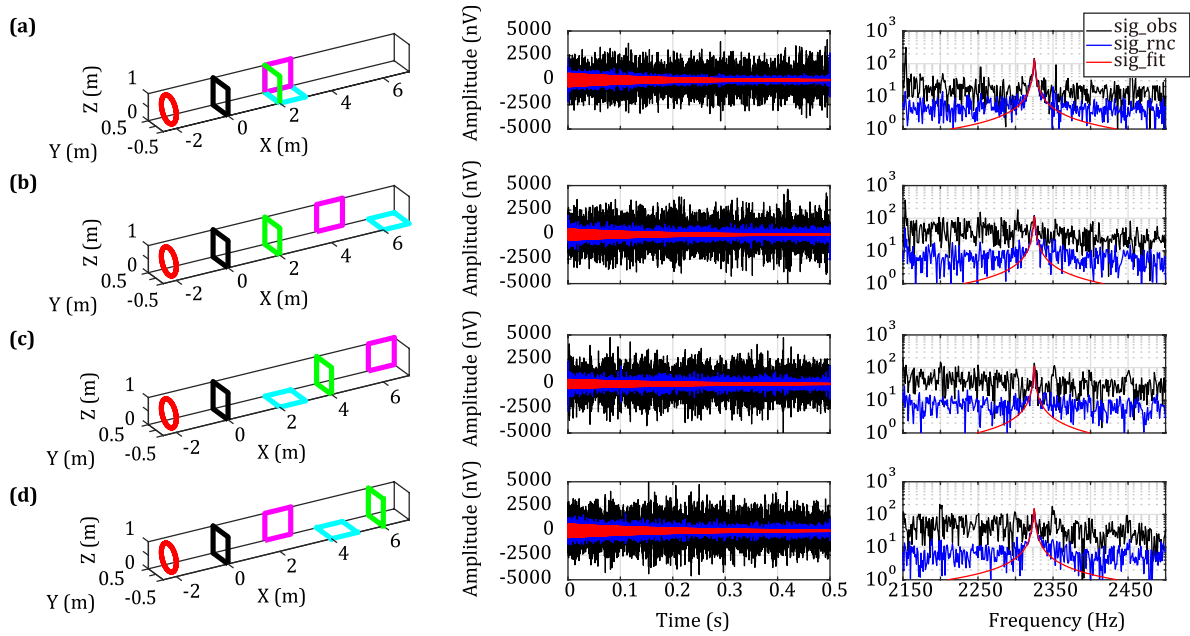


**FIGURE 6.** NRNC processing results of tri-axial reference coil. (a) Non-separation tri-axial reference coil layout, NRNC processing results, and corresponding spectrum. (b) Separation tri-axial reference coil layout 1, NRNC processing results, and corresponding spectrum. (c) Separation tri-axial reference coil layout 2, NRNC processing results, and corresponding spectrum. (d) Separation tri-axial reference coil layout 3, NRNC processing results, and corresponding spectrum.

**D. FACTOR OF TRI-AXIAL REFERENCE COIL AFFECTING NRNC**

A non-separation tri-axial reference coil is used to discuss the degree of influence of the distance between reference coil and detection coil on the NRNC results. The distance is assumed to be 1 – 5 m, the received data in the detection coil are collected, and the estimates of noise level, SNR, and UNMR signal before and after processing are obtained using the NRNC method, as shown in Fig. 7. Fig. 7a presents that the noise level of the received data before processing is close to 1200 nV, and the noise level increases from 168.8 nV to 351.3 nV after processing.

The  $\hat{e}_0$  estimates for the UNMR signal are the same, but the uncertainty increases with the increase in distance, as shown in Fig. 7b. When the distance is 1 m, the  $\hat{e}_0$  estimates are slightly increased because the tri-axial reference coil is close to the detection coil with a mutual inductance. The SNR of the processed data decreases with the increase in distance, and  $\Delta$ SNR drops from 16.7 dB to 10.3 dB. Therefore, when the tri-axial reference coil is close to detection coil, the noise in the received data is relevant and the processing effect of NRNC is strong. However, given the impact of mutual inductance, the distance between the two should be kept at around 2 m.

The output amplitude of the signal generator is changed to test the  $\hat{e}_0$  and  $\hat{T}_2^*$  estimation accuracy of the NRNC method based on the non-separation tri-axial reference coil on UNMR signal and SNR improvement effect. The distance of the non-separation tri-axial reference coil is kept 2 m away from the detection coil. The output current ( $A_{out}$ ) of the signal

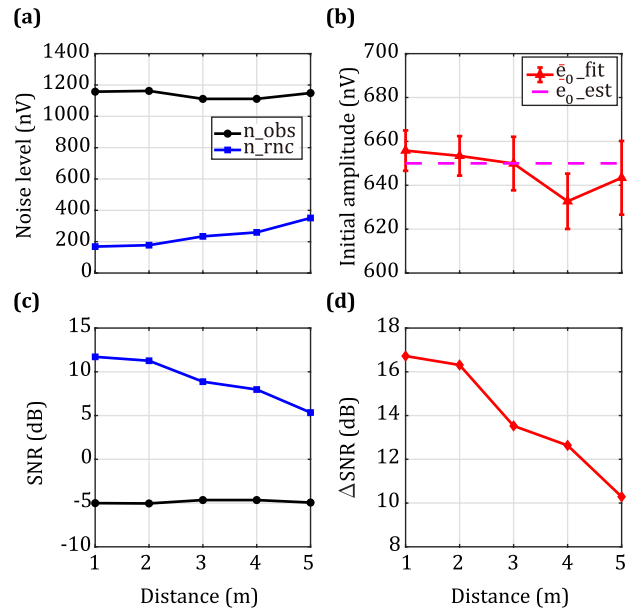


**FIGURE 7.** NRNC processing results of non-separation tri-axial reference coil and detection coil at different distances. (a) Changes in noise levels. (b) Estimates of the UNMR signal  $\hat{e}_0$ . (c) SNR changes. (d) SNR increased value.

generator is gradually decreased from 10 mA to 0.005 mA, and the received data of the detection coil are subjected to NRNC processing to obtain  $\hat{e}_0$  and  $\hat{T}_2^*$  through fitting. Figs. 8a, and b show that the estimate of  $\hat{e}_0$  decreases linearly with the decrease in  $A_{out}$ , the linear relationship (red dotted line) is  $\hat{e}_0 = (|A_{out}| \times 678.95 - 18.9) \times 10^{-9}$  nV, and the



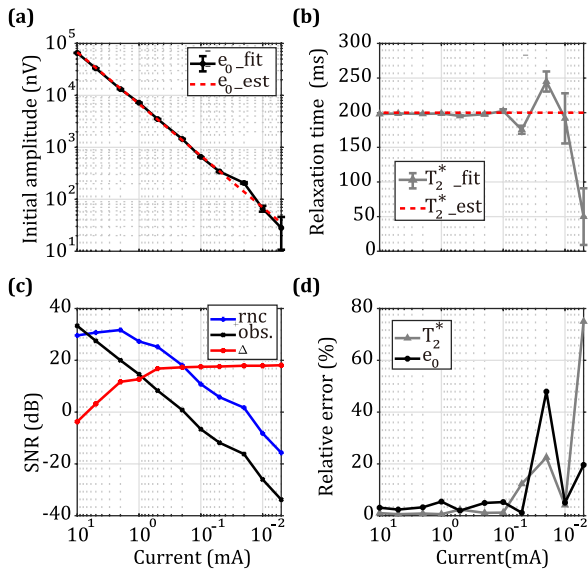


**FIGURE 8.** UNMR signal estimation and SNR comparison results obtained by changing the output current of the signal generator. (a) Estimate of  $\hat{e}_0$ . (b) Estimate of  $\hat{T}_2^*$ . (c) SNR comparison. (d) Relative error of the estimates of  $\hat{e}_0$  and  $\hat{T}_2^*$ .

estimate of  $\hat{T}_2^*$  remains the same. However, when  $A_{out}$  is less than 0.1 mA, the accuracy of the estimates of  $\hat{e}_0$  and  $\hat{T}_2^*$  decreases, and the uncertainty increases. The relative error curve is shown in Fig. 8d. When  $A_{out}$  is less than 0.01 mA,  $\hat{T}_2^*$  has completely deviated from the theoretical value, that is, the parameters of the UNMR signal cannot be reliably extracted. Fig. 8c presents that the SNR of the observed data decreases linearly with the decrease in  $A_{out}$ , whereas the SNR after NRNC processing increases (except  $A_{out} = 10$  mA). Moreover,  $\Delta SNR$  increases with the decrease in the SNR of the observed data. Thus, when the SNR of the observed data is very high, NRNC should not be used; when the SNR of the observed data is low, NRNC should be used. Given that the relevant noise levels in the environment are constant,  $\Delta SNR$  is also limited, with the maximum of 18.1 dB in this case. Therefore, when SNR of a single observed datum is extremely low ( $< -28$  dB), or the SNR is still less than  $-10$  dB after 64 overlays, the accuracy of the extracted  $\hat{e}_0$  and  $\hat{T}_2^*$  is still lower and has large uncertainty even when NRNC is used.

#### IV. DISCUSSION

In a mine or tunnel, the effective reduction in noise determines whether UNMR can be used reliably. The existing noise cancellation method has effectively eliminated or reduced  $V_{spike}$ ,  $V_{harmonic}$ , and  $V_{gauss}$  in the NMR received data [23]. However, some  $V_{uncertain}$  cannot be directly determined and decreased by stacks. The NRNC method proposed in this study targets at this noise type. Compared with the remote reference coil, the nearby reference coil has a stronger correlation with the uncertain system noise of the detection coil and can effectively reduce  $V_{uncertain}$ . As for the problem of coupled UNMR signal in

the nearby reference coil, a two-step solution is proposed. The first step is to calculate the transfer function using the second half of the received data. The second step is to estimate the relevant noise in the detection coil using the first half of the received data in the reference coil. At this time, if an UNMR signal component exists in the noise estimation results, then the non-linear fitting method [24] is used to estimate the UNMR signal parameters and subtract them. In Fig. 4, the SNR of the received data in detection coil through NRNC processing increases significantly, and the UNMR signal is not lost. On the contrary, the UNMR signal after conventional RNC processing is seriously distorted [20]. Fig. 7 shows that, with the increase in distance, the SNR promotion after NRNC processing decreases gradually, and the nearby reference coil is better than the remote reference coil.

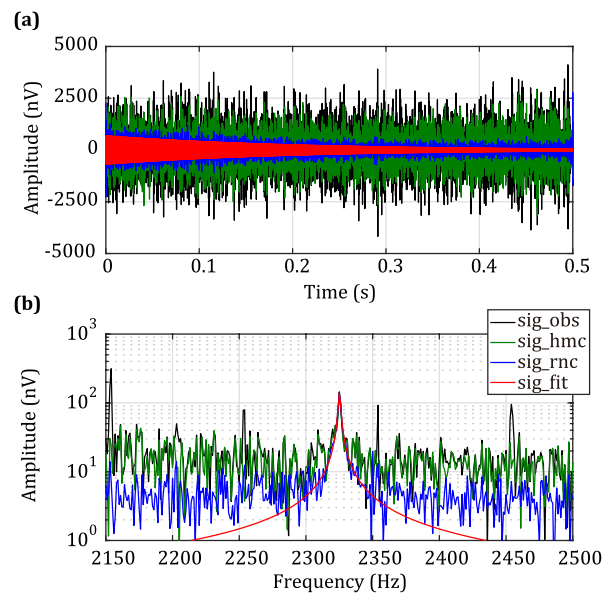


**FIGURE 9.** Comparison of the processing results of NRNC and harmonic modeling. (a) Received data and processing results. (b) Corresponding spectrum.

For  $V_{harmonic}$ , harmonic modeling [10] and RNC [12] are the most commonly used noise cancellation methods. Under the condition of strong underground noise, the processing effect of the two methods is equal, but the harmonic modeling method is better than the RNC method in some cases [20]. The reason is that the RNC uses a remote reference coil, which is less relevant to the noise in detection coil. The NRNC algorithm proposed in this study has a significantly better processing effect than the harmonic modeling method, as shown in Fig. 9. The observed data (black line) and the NRNC processing results (blue line) in Fig. 9 are from Fig. 6a, and the green line is the result after harmonic modeling processing. Harmonic modeling processing can eliminate  $V_{harmonic}$  but not  $V_{uncertain}$ ; thus, the residual noise level is significantly higher than the NRNC processing results. Although the nearby reference coil needs the support of additional coils and multi-channel instruments, a small fixed non-separation

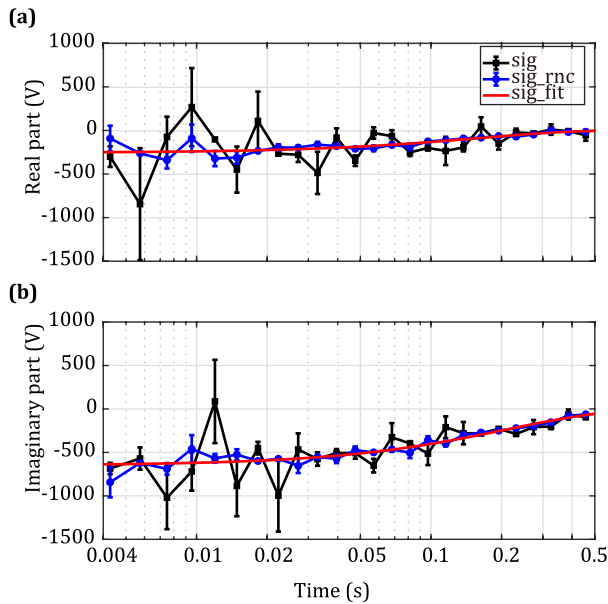


**FIGURE 10.** Received data used for QT inversion are sorted before and after NRNC processing. (a) Real part. (b) Imaginary part.

tri-axial coil can be used in the mine, which is closer to detection coil and can improve SNR greater than 15 dB. The problem of strong noise in the mine then can be solved.

The NRNC can not only greatly improve SNR and the accuracy of UNMR signal estimation but also increase the accuracy of NMR inversion [25]. The most advanced QT inversion method [26] uses all the received data in detection coil instead of the estimates of  $\hat{\epsilon}_0$  and  $\hat{T}_2^*$ . The gate integral method [27] is used to decrease the amount of the received data (the number of gates is usually 30). The results of the received data before and after NRNC processing are shown in Fig. 10. The received data before processing seriously deviate from the results of the UNMR signal fitting and have large uncertainty; the data after processing coincide with the UNMR signal and have small uncertainty. QT inversion uses these gating data and utilizes the uncertainty as the weighted value to constrain the inversion results [23]. Therefore, an accurate, stable, and high-resolution water content distribution is expected to be obtained by inversion using the gating data after NRNC processing.

## V. CONCLUSION

In a mine or tunnel, strong ambient noise restricts the application effect of UNMR advance detection of water sources causing diaster. As for the power line harmonics and uncertain system noise in the received data of the UNMR detection coil, this study proposes a method based on NRNC processing, which greatly improves the data SNR without losing the UNMR signal. Compared with the remote reference coil, the noise obtained by the nearby reference coil is more correlated with the noise in detection coil, which cancels more frequency harmonic and uncertain system noise. Comparison of the influences of the number, direction, and distance of the

reference coil with the detection coil on the results of NRNC processing shows that the optimal choice is to obtain the non-separation tri-axial reference coil. First, the increase in the number of reference coils significantly increases  $\Delta$ SNR. Second, the  $\Delta$ SNR using the non-separation tri-axial reference coil is greater than the coaxial and separation tri-axial reference coil. Third, with the increase in the distance between the reference coil and detection coil,  $\Delta$ SNR decreases gradually. In the measured signal experiment in this study, the SNR after NRNC processing increases up to a maximum of 18 dB. After 64 times of stack, the UNMR signal with the initial amplitude of approximately 660 nV is accurately extracted in the environment with a noise level of  $10^4$  nV. Finally, we obtain a method that has better results based on multiple nearby reference coils and improved RNC than those of conventional remote RNC and power line harmonics through the discussion. The improvement in SNR can not only improve the accuracy of UNMR signal  $\hat{\epsilon}_0$  and  $\hat{T}_2^*$  estimation and reduce the uncertainty but also is expected to improve the resolution and stability of UNMR inversion results.

## REFERENCES

- [1] M. Hertrich, "Imaging of groundwater with nuclear magnetic resonance," *Prog. Nucl. Man. Reson. Spectrosc.*, vol. 53, no. 4, pp. 227–248, Nov. 2008. [Online]. Available: <http://www.sciencedirect.com/science/article/B6THC-4RW434D-1/2/789833a975ca815f7d090897e33d2d77>
- [2] A. Legchenko and P. Valla, "A review of the basic principles for proton magnetic resonance sounding measurements," *J. Appl. Geophys.*, vol. 50, nos. 1–2, pp. 3–19, 2002. [Online]. Available: <http://www.sciencedirect.com/science/article/B6VFC-45FYTYW-1/2/c211d7d370afe56303efad3c79009e1c>
- [3] J. Lin, G. Du, J. Zhang, X. Yi, C. Jiang, and T. Lin, "Development of a rigid one-meter-side and cooled coil sensor at 77 K for magnetic resonance sounding to detect subsurface water sources," *Sensors*, vol. 17, no. 6, p. 1362, 2017.
- [4] S. K. Bharti and R. Roy, "Quantitative  $^1\text{H}$  NMR spectroscopy," *TrAC Trends Anal. Chem.*, vol. 35, pp. 5–26, 2012. [Online]. Available: <http://www.sciencedirect.com/science/article/pii/S0165993612000702>
- [5] M. E. Ladd, P. Bachert, M. Meyerspeer, E. Moser, A. M. Nagel, D. G. Norris, S. Schmitter, O. Speck, S. Straub, and M. Zaiss, "Pros and cons of ultra-high-field MRI/MRS for human application," *Prog. Nucl. Magn. Reson. Spectrosc.*, vol. 109, pp. 1–50, Dec. 2018. [Online]. Available: <http://www.sciencedirect.com/science/article/pii/S007965651830013X>
- [6] A. A. Behroozmand, K. Keating, and E. Auken, "A review of the principles and applications of the NMR technique for near-surface characterization," *Surv. Geophys.*, vol. 36, no. 1, pp. 27–85, Jan. 2015. [Online]. Available: <http://link.springer.com/article/10.1007%2Fs10712-014-9304-0>
- [7] J. M. Greben, R. Meyer, and Z. Kimmie, "The underground application of magnetic resonance soundings," *J. Appl. Geophys.*, vol. 75, no. 2, pp. 220–226, 2011. [Online]. Available: <http://www.sciencedirect.com/science/article/pii/S0926985111001091>
- [8] T. Lin, Y. Yang, X. Yi, C. Jiang, and T. Fan, "First evidence of the detection of an underground nuclear magnetic resonance signal in a tunnel," *J. Environ. Eng. Geophys.*, vol. 23, no. 1, pp. 77–88, Mar. 2018.
- [9] X. Yi, J. Zhang, T. Fan, B. Tian, and C. Jiang, "Design of meter-scale antenna and signal detection system for underground magnetic resonance sounding in mines," *Sensors*, vol. 18, no. 3, p. 848, 2018.
- [10] J. J. Larsen, E. Dalgaard, and E. Auken, "Noise cancelling of MRS signals combining model-based removal of powerline harmonics and multichannel Wiener filtering," *Geophys. J. Int.*, vol. 196, no. 2, pp. 828–836, 2014. [Online]. Available: <http://gji.oxfordjournals.org/content/196/2/828.abstract>
- [11] C. Jiang, J. Lin, Q. Duan, S. Sun, and B. Tian, "Statistical stacking and adaptive notch filter to remove high-level electromagnetic noise from MRS measurements," *Near Surf. Geophys.*, vol. 9, pp. 459–468, Oct. 2011.

- [12] E. Dalgaard, E. Auken, and J. J. Larsen, "Adaptive noise cancelling of multichannel magnetic resonance sounding signals," *Geophys. J. Int.*, vol. 191, no. 1, pp. 88–100, 2012.
- [13] J. J. Larsen, "Model-based subtraction of spikes from surface nuclear magnetic resonance data," *Geophysics*, vol. 81, no. 4, pp. WB1–WB8, 2016.
- [14] B.-F. Tian, J. Lin, Q.-M. Duan, and C.-D. Jiang, "Variable step adaptive noise cancellation algorithm for magnetic resonance sounding signal with a reference coil," *Diqiu Wuli Xuebao*, vol. 55, no. 7, pp. 2462–2472, 2012.
- [15] A. Legchenko and P. Valla, "Removal of power-line harmonics from proton magnetic resonance measurements," *J. Appl. Geophys.*, vol. 53, nos. 2–3, pp. 103–120, 2003. [Online]. Available: <http://www.sciencedirect.com/science/article/B6VFC-49793R2-3/2/2d754130fe97662874dc192cb84126ad>
- [16] R. Ghanati, M. Fallahsafari, and M. K. Hafizi, "Joint application of a statistical optimization process and empirical mode decomposition to magnetic resonance sounding noise cancelation," *J. Appl. Geophys.*, vol. 111, pp. 110–120, Dec. 2014.
- [17] R. Ghanati, M. K. Hafizi, R. Mahmoudvand, and M. Fallahsafari, "Filtering and parameter estimation of surface-nmr data using singular spectrum analysis," *J. Appl. Geophys.*, vol. 130, pp. 118–130, Jul. 2016.
- [18] S. Costabel, "Noise reduction strategy for underground mrs based on a three-component remote reference antenna," in *Proc. 7th Int. Workshop Magn. Reson.*, 2018, pp. 1–4.
- [19] M. Müller-Petke and S. Costabel, "Comparison and optimal parameter settings of referencebased harmonic noise cancellation in time and frequency domains for surface-NMR," *Near Surf. Geophys.*, vol. 12, pp. 199–210, Apr. 2014.
- [20] J. J. Larsen and A. A. Behroozmand, "Processing of surface-nuclear magnetic resonance data from sites with high noise levels," *Geophysics*, vol. 81, no. 4, pp. WB75–WB83, 2016.
- [21] M. H. Levitt, *Spin Dynamics: Basics of Nuclear Magnetic Resonance*. Hoboken, NJ, USA: Wiley, 2002.
- [22] J. O. Walbrecker, M. Hertrich, and A. G. Green, "Off-resonance effects in surface nuclear magnetic resonance," *Geophysics*, vol. 76, no. 2, pp. G1–G12, 2011. [Online]. Available: <http://link.aip.org/link/?GPY/76/G1/1>
- [23] M. Müller-Petke, M. Braun, M. Hertrich, S. Costabel, and J. Walbrecker, "MRSMATLAB—A software tool for processing, modeling, and inversion of magnetic resonance sounding data," *Geophysics*, vol. 81, no. 4, pp. WB9–WB21, May 2016. doi: [10.1190/geo2015-0461.1](https://doi.org/10.1190/geo2015-0461.1).
- [24] A. Legchenko and P. Valla, "Processing of surface proton magnetic resonance signals using non-linear fitting," *J. Appl. Geophys.*, vol. 39, no. 2, pp. 77–83, 1998. [Online]. Available: <http://www.sciencedirect.com/science/article/B6VFC-3V5M2GS-7/2/92e693c8c6cf55a760b76875255db2e7>
- [25] C. Jiang, M. Müller-Petke, J. Lin, and U. Yaramanci, "Magnetic resonance tomography using elongated transmitter and in-loop receiver arrays for time-efficient 2-D imaging of subsurface aquifer structures," *Geophys. J. Int.*, vol. 200, no. 2, pp. 824–836, 2015. [Online]. Available: <http://gji.oxfordjournals.org/content/200/2/824.abstract>
- [26] M. Müller-Petke and U. Yaramanci, "QT inversion—Comprehensive use of the complete surface NMR data set," *Geophysics*, vol. 75, no. 4, pp. WA199–WA209, 2010. [Online]. Available: <http://link.aip.org/link/?GPY/75/WA199/1>
- [27] A. A. Behroozmand, E. Auken, G. Fiandaca, A. V. Christiansen, and N. B. Christensen, "Efficient full decay inversion of MRS data with a stretched-exponential approximation of the distribution," *Geophys. J. Int.*, vol. 190, no. 2, pp. 900–912, 2012. doi: [10.1111/j.1365-246X.2012.05558.x](https://doi.org/10.1111/j.1365-246X.2012.05558.x).



**JIAN ZHANG** received the B.S. degree in biomedical engineering from the Changchun University of Science and Technology, Changchun, China, in 2009. He is currently pursuing the Ph.D. degree in measurement technology and instruments with the College of Instrumentation and Electrical Engineering, Jilin University.

His research interest includes surface and underground nuclear magnetic resonance instruments.



**GUANFENG DU** received the B.S. degree in software from Hunan University, Changsha, China, in 2010. He is currently pursuing the Ph.D. degree in measurement technology and instruments with the College of Instrumentation and Electrical Engineering, Jilin University.

His research interest includes surface and underground nuclear magnetic resonance sensors and instruments.



**JUN LIN** received the B.S. and M.S. degrees in applied geophysics from the Changchun College of Geosciences, Changchun, China, in 1982 and 1987, respectively.

In 1989, he was a Visiting Scholar with the University of Leicester, Leicester, U.K. In 1996, he was a Senior Scholar with The University of Arizona, Tucson, AZ, USA. Since 2005, he has been with the College of Instrumentation and Electrical Engineering, Jilin University, Changchun,

as a Chairman. He is currently a Professor with Jilin University. He has finished 13 national projects and received 2 key national invention awards as the Chief Director. He has authored 10 books and more than 300 papers, and holds 50 patents. His research interests include seismic instrument, nuclear magnetic resonance instrument, and time and frequency domain electromagnetic instrument developments, and geophysical modeling process.



**XIAOFENG YI** received the B.S. and M.S. degrees in electrical theory and new technology and the Ph.D. degree in measuring and testing technology and instrument from Jilin University, Changchun, China, in 2008, 2010, and 2014, respectively.

He is currently a Lecturer with the College of Electrical Engineering and Instrumentation Technology, Jilin University. His research interest includes underground nuclear magnetic resonance instruments.



**CHUANDONG JIANG** received the B.S. degree in measuring and controlling technology and instrument and the M.S. and Ph.D. degrees in measuring and testing technology and instrument from Jilin University, Changchun, China, in 2007, 2009, and 2013, respectively. From 2016 to 2018, he held a visiting postdoctoral position with the Leibniz Institute of Applied Geophysics, Hannover, Germany.

He is currently an Associate Professor with the College of Instrumentation and Electrical Engineering, Jilin University. His research interests include instrument developing, data processing, and 2D and 3D inversion of surface nuclear magnetic resonance.

...